

Analytical investigation to the bending strength-deformation characteristics of the piers of Khilgaon Flyover in Dhaka

M. A. Kader and M. M. Hoque

*Department of Civil Engineering
Dhaka University of Engineering and Technology, Gazipur, Bangladesh*

Received on 29 October 2009

Abstract

Bending strengths-deformation characteristics of the piers of Khilgaon have been investigated analytically by taking the nonlinearity of the material into consideration. The bottom most sections of the piers, the most critical sections in pier under bending, are used in the analysis. To achieve the goal, nonlinear sectional analyses of the reinforced concrete (RC) piers are carried out using fiber model of RC cross-sections. Moment-curvature relationships are found from the sectional analysis results. Yield moments, ultimate moments, and yield curvatures and ultimate curvatures are obtained from moment-curvature relationships. An elastic perfectly plastic model for reinforcing steel and a well recognized nonlinear constitutive model for concrete incorporating the effect of confinements has been used in the analysis. The effect of axial force on the moment strength has been investigated.

© 2009 Institution of Engineers, Bangladesh. All rights reserved.

Keywords: Fiber model, sectional analysis, moment strength, curvature and ductility.

1. Introduction

Bangladesh is an earthquake prone country. The earthquakes are of stochastic nature. Due to existence of active faults, there is a high probability of occurrence of a large magnitude earthquake (Ali and Chowdhury, 1994; 1992) in Bangladesh. It is, therefore, necessary to predict the probable losses due to future earthquakes, to assess the seismic safety, to make plan for seismic retrofitting, pre-earthquake and disaster mitigating plan. One of the ways to assess probable losses under an earthquake is to investigate the seismic vulnerability of structures. Seismic vulnerability can be assessed in two ways: empirically and analytically. Empirical vulnerability analyses are virtually impossible for Bangladesh, since structural damage data due to earthquakes are not available. Hence, analytical vulnerability analysis is the only choice to be made for obtaining

vulnerability of structures. Lateral strengths and deformation characteristics of structures are obtained for carrying out analytical vulnerability of structures.

Among different types of structures bridges are of vital importance due to the contribution offered in transportation. Flyover is one kind of bridge structures that are being constructed to reduce remarkable traffic congestion of mega city Dhaka. Two flyovers namely Mohakhali flyover and Khilgaon flyover have already been constructed in Bangladesh. Khilgaon is the second one between them. The seismic safety or vulnerability analyses have not yet been conducted for such type of bridge structures in Bangladesh.

Further, the capacity design concept is a strong improvement in seismic structural reliability and adopted by several design specifications (JRA, 2002, CalTrans, 1999), uses more realistic method for ensuring minimum loss due to an earthquake. According to the concept, the position and extent of damage is restricted. In order to ensure the position of damage, the plastic components are chosen in such a way that suitable plastic mechanism can be formed. An appropriate design shall guarantee sufficient ductile behavior of the plastic components. According to design specifications of Highway Bridges in Japan (JRA, 2002, 1998), the damage in pier is admissible as well as repairable in a bridge structure. Referring many references, Karim and Yamazaki (2000) cited that the bridges constructed in recent days do not suffer shear failure which is unexpected in bridge structures. Hence, it is believed that the piers will fail, if so, in bending due to a large magnitude earthquake. Therefore, the bending strengths of the piers in bending are to be evaluated to verify the seismic performance of the flyover. Different piers with same cross-section may be under different loads from super structure; and the axial load effects the bending deformation characteristic largely. To obtain the moment-curvature relationship and the behavior of RC bridge pier in bending Memari et al. (2005), and Priestley and Park (1987) have carried out similar investigations for the bridge piers.

On the basis of the background, the study aims at obtaining the bending strength-deformation characteristics of the piers by carrying out nonlinear sectional analyses. The bending strengths are presented in the form of yield moment and ultimate moment and their associated curvatures. The ultimate bending strengths of the piers are compared by normalizing the strengths by load on the pier and their height. The effect of axial force on the moment strength has also been investigated.

1.1 Brief description of Khilgaon Flyover and the piers

To ease the nagging traffic congestion in the city center, the country's second and biggest fly-over was constructed at the busy road-rail intersection near Khilgaon, connecting Rajarbagh in the south, Malibagh in the west and Sayedabad in the east. According to the Local Government Engineering Department (LGED), people of the eastern region of Dhaka had to lose three and a half hours everyday, as the rail crossing would close around 72 times a day to allow passage of trains. Those people are now able to move without much delay.

Construction of the 1.9 km long and 14 meters wide flyover, having 543 piles, began in 2001 at a cost of Tk 81.75 crore, including expenses for land acquisition and compensation to the affected people. The flyover has a 780-metre main bridge and three ramps. The length of the flyover towards Sayedabad is 303 metres, Malibagh 190 metres and Rajarbagh 285 metres. The ramp towards Sayedabad is 220 metres, Malibagh 202 metres and Rajarbagh 222 metres. The LGED built and opened to traffic in March 2005.

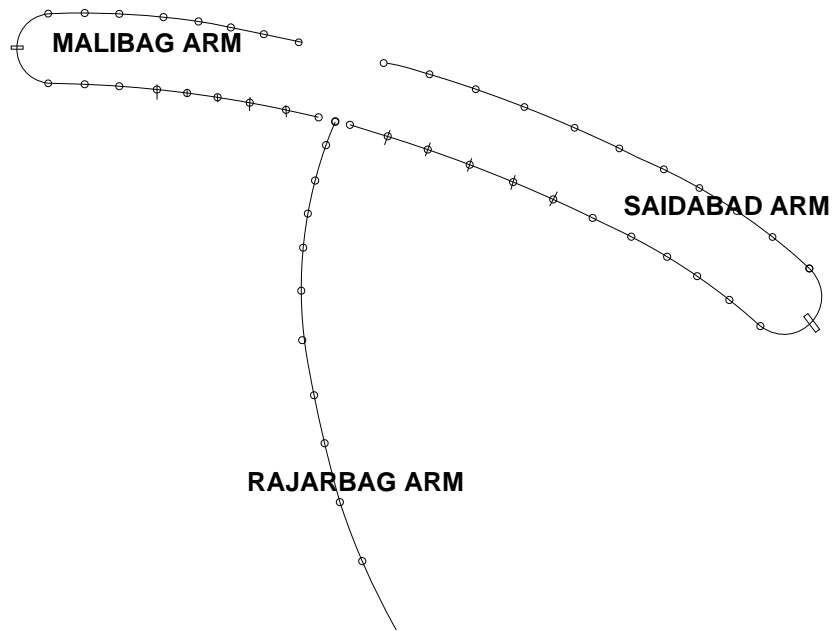


Fig. 1.1 Piers layout of Khilgaon flyover

The whole structure is of concrete girder with slab. The range of span lengths is 16.0 meters to 28 meters. The piers of flyover are of circular shape having of two different diameters: 1.5 meters and 2.0 meters, and are of with hammerhead type. The elevation and cross-section of a typical pier is shown in Fig. 1.2. The piers heights above the pile cap vary from 6.35 meters to 11.72 meters. The height, sectional dimensions, longitudinal reinforcement, transverse reinforcement is presented in tabular form in Table1.

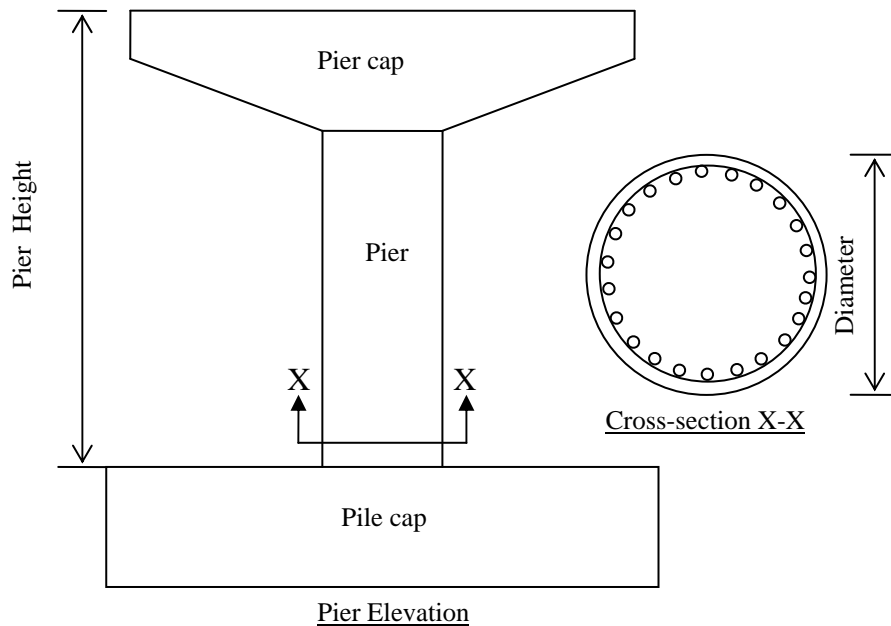


Fig. 1.2. Elevation and Cross-section of a typical pier of Khilgaon flyover

Table-1
Piers of Khilgaon flyover

Pier ID	Pier height (m)	Diameter (m)	Longitudinal reinforcing steel ratio (%)	Volumetric ratio of transverse steel (%)
PML03 to PML05	6.844 to 8.658	1.5	1.61	0.30
PML06 to PML08 and PML13	9.650 to 11.081	1.5	2.64	0.30
PML11, PML14	11.723 to 11.276	1.5	2.82	0.30
PML12, PML15, PML16	9.731, 8.732	1.5	2.28	0.30
PR02 to PR12	6.386 to 7.888	2.0	0.91	0.22
PS02 to PS10	7.292 to 7.424	2.0	0.91	0.22
PM02 to PM07	6.351 to 7.286	2.0	0.91	0.22

2. Materials and methods

2.1 Materials properties

The strength-deformation characteristics of the piers depend largely on the stress-strain relationship of the constituents' material. Material strengths are obtained from the design data. The design strengths are: $f'_c = 25$ MPa; yield strength of reinforcing steel, $f_y = 60$ ksi. The modulus of elasticity of concrete and reinforcing steel used in the study are $E_c = 23667$ MPa and 200000 MPa, respectively.

2.1.1 Constitutive model of materials

Sectional properties of the piers are related to the characteristics of the materials i.e., stress-strain relationship and strength of materials. For particular material strengths of reinforcing steel and concrete, the moment-curvature relationship of a specific section may vary for different constitutive relations. For this reason, a reasonably accurate prediction model for stress-strain relationship of the materials has been a great challenge over the years. In the early days, the stress-stress relationships for unconfined concrete (Wang at al., 1978; Ahmad and Shah, 1982) had been used. With the advancement of experimental facilities, along with experimental investigation, the effect of confinement is now available in literatures (Mander et al., 1988a, 1988b, Hoshikuma et al., 1997). One such model, which has been used extensively in recent years, was developed by Hoshikuma et al. (1997). The descending branch of the material law as well as the increase of strength and corresponding strain because of a confining reinforcement is taken into consideration which is shown in Fig. 2.1. The authors have provided some insight into the behavior of spiral columns under axial and flexural loading. The model stress-strain curve consist the three parts i.e., an ascending branch, falling branch, and sustaining branch. The stress-strain curve can be expressed by the equation shown in below.

$$f_c = \begin{cases} E_c \varepsilon_c \left\{ 1 - \frac{1}{n} \left(\frac{\varepsilon_c}{\varepsilon_{cc}} \right) \right\} & (0 \leq \varepsilon_c \leq \varepsilon_{cc}) \\ f_{cc} - E_{des} (\varepsilon_c - \varepsilon_{cc}) & (\varepsilon_{cc} < \varepsilon_c \leq \varepsilon_{cu}) \end{cases} \quad (2.1)$$

where n = coefficient, E_{des} = deterioration rate, and are given as

$$n = \frac{E_c \epsilon_{cc}}{E_c \epsilon_{cc} - f_{cc}} \tag{2.2}$$

$$E_{des} = 11.2 \frac{f_{co}^2}{\rho_s f_{yh}} \tag{2.3}$$

The confinement effectiveness for circular sections may be represented as

$$f_{cc} = f_{co} + 3.8\alpha\rho_s f_{yh} \tag{2.4}$$

$$\epsilon_{cc} = 0.002 + 0.033\beta \frac{\rho_s f_{yh}}{f_{co}} \tag{2.5}$$

in which α and β = modification factors depending on confined sectional shape: for circular $\alpha = 1.0$ and $\beta = 1.0$; for square $\alpha = 0.2$ and $\beta = 0.4$.

The graphical presentation of the Hoshikuma et al. [1997] model is given as below:

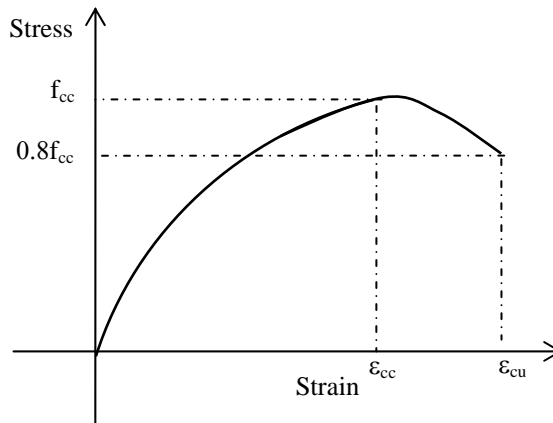


Fig. 2.1. Constitutive model of concrete

The elastic perfectly plastic model for reinforcing steel is used in the study. The yield strength is taken as the design yield strength used in the design. The modulus of elasticity of reinforcing steel considered in the study is 2×10^5 MPa. The ultimate strain used is 0.01 mm/mm. A constitutive model of reinforcing steel is shown in Fig.2.2.

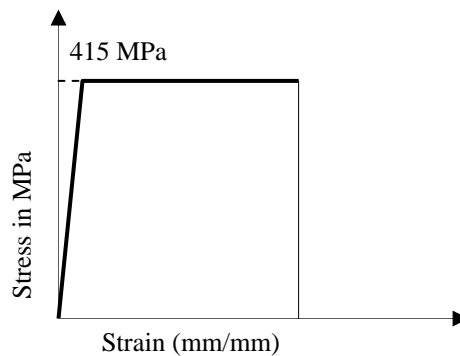


Fig. 2.2. Constitutive model of reinforcing steel

2.3 Sectional analysis

As mentioned earlier sectional analysis are carried out by discretizing a RC section into several segments or fibers. In the analysis, the mechanical behavior of a section is analyzed in fiber model using the constitutive relationships of the material, and taking the equilibrium and kinematics into considerations.

2.3.1 Fiber model

The fiber model is based on the assumptions that the deformed sections remain plain, the shear deformations are neglected; constitutive model of materials are known. In preparing the fiber model, the reinforced concrete cross-section is divided into a number of discrete fibers. The number of fibers is taken around fifty which is recommended by design specifications (JRA, 2002). Same model has adopted by Parche (2000) in their investigation to simulate the cross-sectional behavior. First of all, a number of extreme compressive strains starting from small value to ultimate compressive strain are assumed.

2.3.2 Sectional analysis methodology

For the assumed extreme compressive strains, the depth of neutral axis is determined from the equilibrium of axial force. Having computed the strain of each fiber for a particular extreme strain, the corresponding stresses are determined using the constitutive model of the material. Integration of the stresses gives the resulting internal forces. The moment capacity corresponding to each neutral axis depth is then plotted versus the curvature. The process can continue until the ultimate compressive strain of concrete. The overall procedure can be summarized as,

- 1) The material properties and the constitutive model of concrete and reinforcing steel are selected first
- 2) The bending moment and curvature at cracking of concrete, and bending tension strength of concrete are computed by using the following equations:

$$M_c = W_i \left(f_{bt} + \frac{N_i}{A_i} \right) \quad (2.6)$$

$$\phi_c = \frac{M_c}{E_c I_i} \quad (2.7)$$

$$f_{bt} = 0.23 f_{ck}^{2/3} \quad (2.8)$$

where

M_c : Bending moment at cracking (N-mm)

ϕ_c : Curvature of cracking (1/mm)

W_i : Sectional modulus of pier having considered the axial reinforcement in the i -th section from the height of the super structural inertia force (mm^3)

f_{bt} : Bending tensile strength of concrete (N/mm^2)

N_i : Axial force due to the weights of superstructure and substructure acting on the i -th section from the height of the super structural inertia force (N).

A_i : Section area of pier having considered the axial reinforcement in the i -th section from the height of the super structural inertia force (mm^2)

E_c : Young's modulus of concrete (N/mm^2)

I_i : Moment of inertia of pier having considered the axial reinforcement in the i -th section from the height of the super structural inertia force (mm^4)

f_{ck} : Characteristic strength of concrete, but design strength has been used in the investigation. (N/mm^2)

- 3) The section of each element is divided into n divisions in the direction in which inertial force acts, and on the assumption that fiber strain is in proportion to the distance from the neutral axis obtained by assuming that the plane is preserved and the stresses corresponding to the fiber strain are fixed within the respective infinitesimal elements, a neutral axis to satisfy the equilibrium condition of Eq.(2.9) is obtained by trial calculation. The number of divisions in each section is kept within 50.

$$N_i = \sum_{j=1}^n \sigma_{cj} \Delta A_{cj} + \sum_{j=1}^n \sigma_{sj} \Delta A_{sj} \quad (2.9)$$

where

σ_{cj}, σ_{sj} : Stresses of concrete and reinforcement within the j -the infinitesimal part (N/mm^2)

$\Delta A_{cj}, \Delta A_{sj}$: Sectional areas of concrete and reinforcement within the j -the infinitesimal part (mm^2)

After the position of the neutral axis is determined, bending moment and curvature are obtained respectively by Eq.(2.10) and Eq. (2.11)

$$M_i = \sum_{j=1}^n \sigma_{cj} x_j \Delta A_{cj} + \sum_{j=1}^n \sigma_{sj} x_j \Delta A_{sj} \quad (2.10)$$

$$\phi_i = \varepsilon_{co} / x_o \quad (2.11)$$

where

M_i : Bending moment acting on the i -th section from the height of the super structural inertia force (N-mm)

ϕ_i : Curvature of the i -th section from the height of the super structural inertia force (1/m)

x_j : Distance from concrete or reinforcement in the j -the infinitesimal part to the centroid position of section (mm)

ε_{co} : Compressed edge strain of concrete (mm/mm)

x_o : Distance from the compressed edge of concrete to the neutral axis (mm)

Bending moment and curvature formed when the strain occurred in axial tension reinforcement arranged on the outermost edge of the section reaches yield strain ε_{sy}

are obtained and taken as initial yield moment M_{yo} and initial yield curvature ϕ_{yo} .

Besides, the bending moment and curvature formed when the strain of concrete at the position of axial compression reinforcement on the outermost edge reaches ultimate strain ε_{cu} are taken respectively as ultimate bending moment M_u and ultimate curvature ϕ_u .

- 4) Yield curvature ϕ_y in the skeleton curve is calculated by equation (2.12)

$$\phi_y = \left(\frac{M_u}{M_{yo}} \right) \phi_{yo} \quad (2.12)$$

In the current study a finite element based program RESPONSE 2000 (Bentz, 2000) has been used.

2.3.3 Ductility evaluation

Ductility is a mechanical property used to describe the extent to which materials can be deformed plastically without fracture. Larger ductility is expected for all the structures. Ductility largely depends on the expected mode of failure: shear failure and bending failure. Ductility under bending failure is investigated in the study. The ductility is of two types: curvature ductility and displacement ductility. Displacement ductility can be related to curvature ductility. In the study, curvature ductility is estimated in terms of ultimate and allowable ductility. Ultimate curvature ductility is defined as the ratio of ultimate curvature to yield curvature and the allowable ductility is obtained (JRA, 2002, 1998) by equation (2.13)

$$\mu_a = 1 + \frac{\phi_u - \phi_y}{\alpha \phi_y} \quad (2.13)$$

where μ_a : Allowable curvature ductility of the RC pier, ϕ_u : Ultimate curvature of the RC pier, ϕ_y : Yield curvature of the RC pier and α : Safety factor, 3.0 is used in the study.

3. Results and discussion

The bending strengths and curvatures at yielding and ultimate states are obtained from moment-curvature relationships. The moment-curvature relationships are obtained from sectional analyses results. As stated earlier, and presented in Table 1, five different cross-sections at bottom of the pier have been used in the flyover, those have been analyzed using fiber model. The moment-curvature relationships thus obtained are presented in Fig. 3.1. The effect of axial forces on the moment-curvature relation and hence, on the bending strength and curvatures is presented in Fig.3.2. The characteristic moments and curvatures are listed in Table 3. Ultimate and allowable ductility of the piers have been evaluated using yield and ultimate curvature and presented in Fig.3.3. Finally, the bending strengths in terms of horizontal force and superstructures' weight are obtained based on the assumption that the pier with super-structure can be modeled as a single-degree of freedom system.

3.1 Moment-curvature relationships

The moment-curvature relationships of five different RC sections at pier bottom are presented in Fig.3.1.

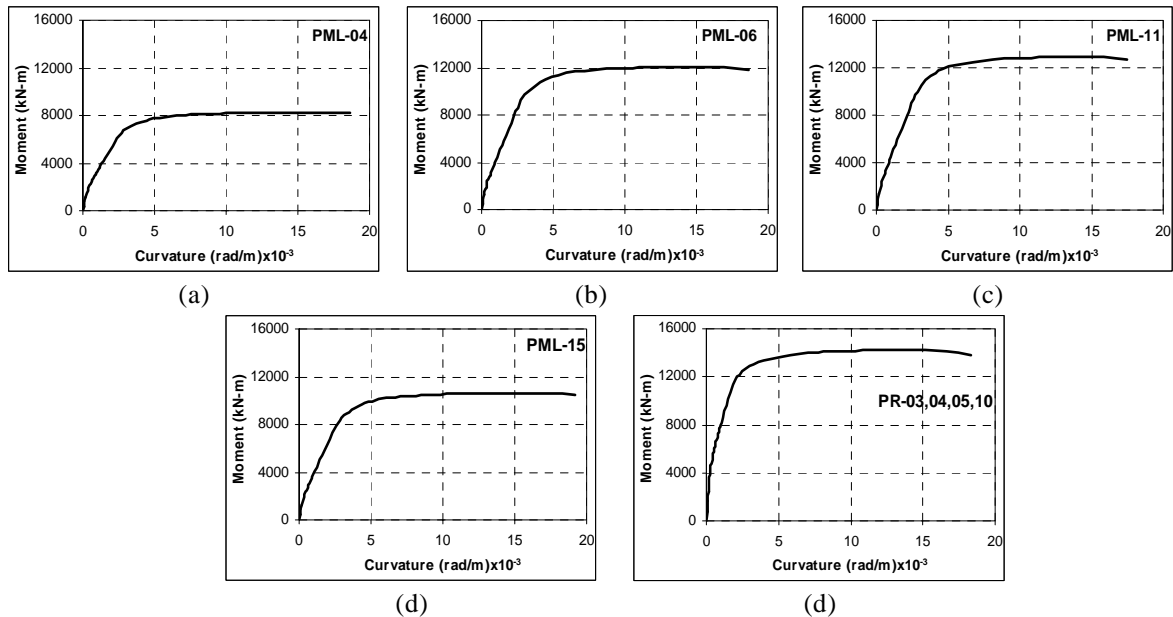


Fig. 3.1. Moment-curvature relationship of the piers bottom sections

It is seen from Fig.3.1 that the moment is found to increase rapidly with increasing curvatures initially, while the rate of increase becomes insignificant after an interval. The reason for changing the relation is that reinforcing steel in the extreme tensile layer reaches yield strength. The moment in the stage is termed as yield moment. Moments are observed to increase further with curvature beyond the yield moment due to the fact that the reinforcement in layers other than in extreme layers is yet to reach yield strength. Further, a minor change in the slope is observed in the initial linear regime. It is due to developing tension cracks in the cover concrete, and hence reduction of effective cross-sectional area occurs. It is also seen that the trend of moment-curvature relationships are for the section same but the slopes, and the characteristic points are found different for different pier cross-sections. The characteristic moment are termed as yield moment and ultimate moment.

It is found from the figures that the moment curvature relation changes with the change in diameter of the pier. For piers of particular diameter, the yield and ultimate moment increase with the increase of longitudinal reinforcement of the pier. Moreover, the slope of the initial regime increases with the increase of longitudinal reinforcement. Very large stiffness can be seen for pier of larger diameter.

3.2 Effect of axial load on moment-curvature relationship

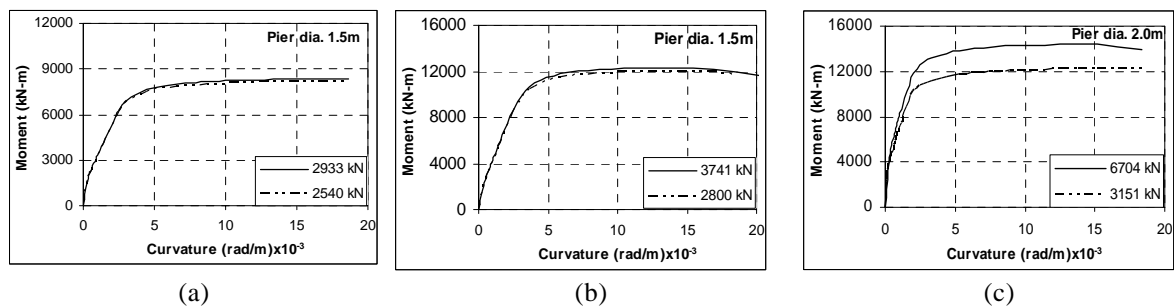


Fig. 3.2. Effect of axial load on moment-curvature relationship of the pier sections

As mentioned earlier, there are seventy two piers with five different cross-sections. The piers are of different height. Due to structural configuration, the loads from the superstructure on the pier are different. Piers with identical cross-section and reinforcement are subjected to different axial loads. Since, the axial load compressed the section, the moment curvature relation are supposed to be different for identical pier-section with different axial loads. To verify the fact, sectional analyses have been carried out for evaluating the effect of axial force on the moment-curvature relationship.

The effect of axial force on the moment-curvature relations can be seen from Fig. 3.2. A larger yield moment capacity is observed for larger axial force. In addition, the larger difference in axial force in compression the larger difference in moment strength. This is due to existence compressive strain in the section due to axial force applying flexural moment. Significant difference in axial force of the pier yield difference in moment strength not so significantly. For instance, for a 112.75% increase in axial force 18.41% increase in ultimate moment can be seen from the figure. With the axial force the stiffness can also be found to increase in the figure shown.

3.3 Characteristic strengths and deformations of the piers

Table 2
Yield and ultimate moment, yield and ultimate curvature to the flyover

Pier ID	Yield Moment (kN-m)	Ultimate Moment Mu (kN-m)	Yield Curvature (rad/m) $\times 10^{-3}$	Ultimate Curvature (rad/m) $\times 10^{-3}$
PML03	6516	8170	3.47	40.82
PML04	6588	8273	2.87	39.13
PML05	6625	8326	2.87	38.39
PML06	9232	12066	3.07	38.49
PML07	9385	12309	3.34	34.69
PML08	10340	12891	3.23	27.69
PML11	10490	12883	3.24	36.02
PML12	8769	10675	3.18	39.08
PML13	9184	11989	3.07	39.63
PML14	9209	12661	3.15	39.84
PML15	7921	10637	3.04	39.81
PML16	7921	10637	3.04	39.81
PR02	11895	14374	2.11	27.30
PR03	11787	14217	2.13	28.01
PR04	11787	14217	2.13	28.01
PR05	11787	14217	2.13	28.01
PR06	11305	14180	2.00	28.18
PR07	11305	14180	2.00	28.18
PR08	11362	14269	2.00	27.76
PR09	11362	14269	2.00	27.76
PR10	11787	14217	2.13	28.01
PR11	11386	14301	2.00	27.63
PR12	10241	12643	1.99	35.84
PS02	9917	12195	1.97	36.27
PS03	10875	13546	2.11	31.39
PS04	10875	13546	2.11	31.39
PS05	10875	13546	2.11	31.39

Pier ID	Yield Moment (kN-m)	Ultimate Moment Mu (kN-m)	Yield Curvature (rad/m)x10 ⁻³	Ultimate Curvature (rad/m)x10 ⁻³
PS06	10807	13451	2.09	31.80
PS07	10807	13451	2.09	31.80
PS08	10807	13451	2.09	31.80
PS09	10807	13451	2.09	31.80
PS10	10807	13451	2.09	31.80
PM02	10875	13546	2.11	31.39
PM03	10875	13546	2.11	31.39
PM04	10875	13546	2.11	31.39
PM05	10875	13546	2.11	31.39
PM06	10875	13546	2.11	31.39
PM07	10875	13546	2.11	31.39

The yield moment, ultimate moment, yield curvature and ultimate curvature of the piers are presented in Table 2. It is found from Table 2 that the yield and the ultimate moments are different for the different pier-sections and the different reinforcement. The ultimate moment moments in same section of the piers are different for different axial forces Mean and coefficient of variation of the yield moments is 10263 kN-m, 14% and ultimate moments is 12841 kN-m, 13%, respectively. Larger variations in yield moments are observed due to the fact that the yield moments are more sensitive to the factors affecting the moment strength.

It is also seen that the yield and ultimate curvatures are different due to the different cross-sections and different reinforcements.

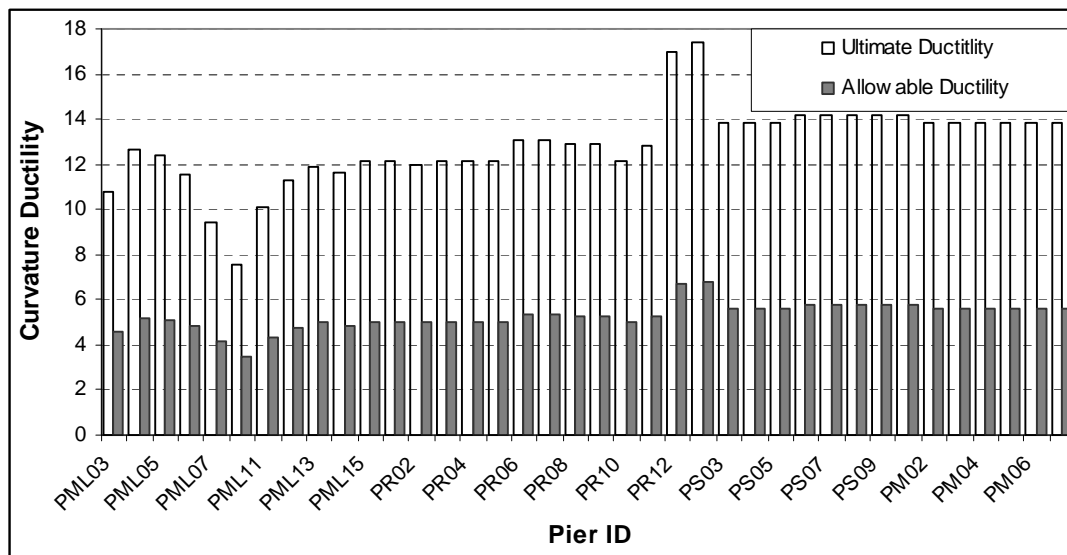


Fig. 3.3. Ultimate and Allowable Curvature Ductility

The ultimate and allowable curvature ductility is presented in Fig. 3.3. It can be seen that the ultimate and allowable curvature ductility is different for different cross-section and reinforcement in piers. It is also seen that the ductility of the pier with same cross-section and reinforcement have been different, and that might be due to the difference in axial load. Mean of the ultimate curvature ductility and the coefficient of variation are 12.87, 14% and for allowable curvature ductility, it is 5.29, 11%, respectively.

3.3 Lateral strengths

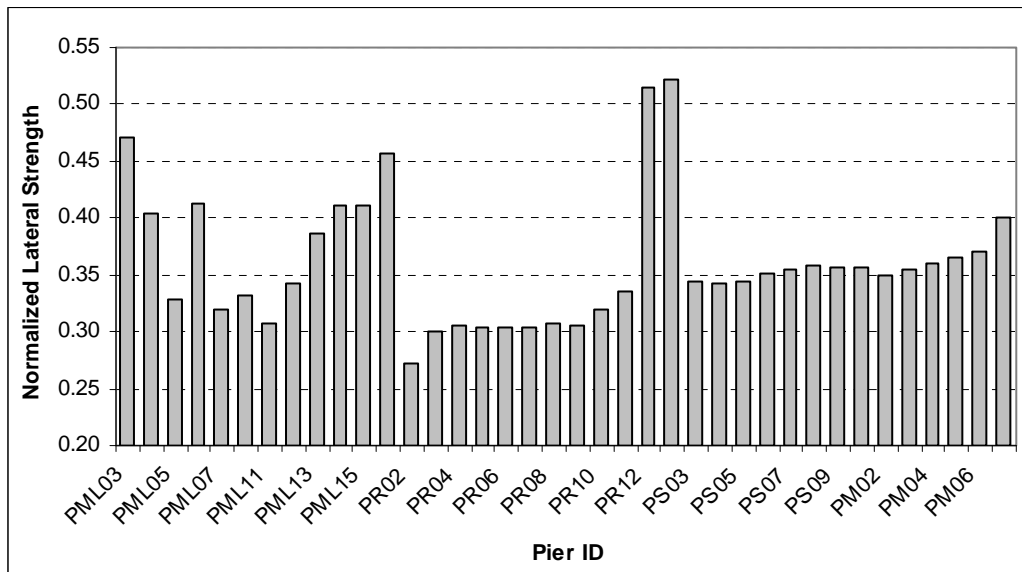


Fig. 3.4. Normalized lateral strength of the piers

The lateral strength in bending is obtained, assuming the pier with super-structure as a single degree of freedom system, from the moment-curvature relationships. The superstructure weight is modeled as inertia force at pier top. The ultimate lateral strengths in bending are used.

The variability of lateral strengths, thus obtained, is presented in Fig. 3.4. It can be seen that the lateral load carrying capacity in flexure varies from 0.272 to 0.522. Mean and standard deviation of the normalized lateral strength is 0.36, 0.058. No specific trend is obtained for the normalized lateral strength in bending and pier height.

4.0 Conclusions

Bending strengths of the piers of Khilgaon flyover are obtained by carrying out nonlinear sectional analyses. Moment-curvature relationship of pier bottom sections are obtained at first step, the characteristic moments: yield moment, ultimate moments, are obtained in the subsequent steps.

The bending capacity of the piers is found to increase with increasing axial force in compression. However, the increase is insignificant. It is also found that the ductility is increasing with decreasing the axial force on pier. The mean and standard deviation value of the ultimate curvature ductility is 12.87, 1.79 and allowable curvatures ductility is 5.29, 0.60 respectively.

The horizontal strengths of the pier in bending are obtained by normalizing the respective moments. It is found that the normalized lateral strengths of the pier in bending lie within the range 0.272 to 0.522. The mean and standard deviation value of the normalized lateral strength is 0.36, 0.058.

References:

Ahmad, S. H. and S. P. Shah.1982. "Complete triaxial stress-strain curves of concrete." Journal of Structural Division, ASCE, 108(4), pp. 728-742.

- Ali, M. H. and J. R. Choudhury. 1994. "Seismic Zoning of Bangladesh", Paper presented at the International Seminar on Recent Developments in Earthquake Disaster Mitigation, Institute of Engineers, Dhaka.
- Ali, M. H. and J. R. Choudhury. 1992. "Tectonics and Earthquake Occurrence in Bangladesh", Paper presented at 36th Annual Convention of the Institution Engineers, Dhaka, Bangladesh.
- Bentz, E. C and M. P. Collins. 2000. Software program for Load-Deformation response of reinforced concrete sections.
- Caltrans, 1999. Seismic Design Criteria, Ver 1.1, California Department of Transport, Sacramento, CA., USA.
- Eurocode, 1994. Design Provisions for Earthquake Resistance of Structures, ENV 1998-2, Bridges. CEN, Brussels.
- Hoshikuma, J., K. Kawashima, K. Nagaya and A. W. Taylor. 1997. "Stress-strain model for confined reinforced concrete in bridge piers." *Journal of Structural Engineering*, pp. 614-633.
- JRA, 1998. Specifications for highway bridges, Part V: Seismic Design, Japan Roadway Association.
- JRA, 2002. Specifications for highway bridges, Part V: Seismic Design, Japan Roadway Association.
- JSCE, 2000. Earthquake resistant design codes in Japan, Japan Society of Civil Engineers.
- Karim, K. R. and Yamazaki, F. 2000. Comparison of empirical and analytical fragility curve of highway bridge piers, *Bulletin of Earthquake Resistant Structure Research center, Institute of Industrial Science, University of Tokyo*, 33:117-128
- Mander J. B., M. J. N. Priestley and R. Park. 1988a. "Theoretical stress-strain model for confined concrete. *Journal of Structural Division, ASCE*, 114(8): pp. 1804-1826.
- Mander J. B., M. J. N. Priestley and R. Park. 1988b. "Observed stress-strain behavior of confined concrete." *Journal of Structural Division, ASCE*, 114(8): pp. 1827-1849.
- Memari, A. M., H. G. Harris, A. A. Hamid and A. Scanlon. 2005. "Ductility evaluation for typical existing RC bridge columns in the eastern USA., *Engineering Structures*, 27, pp. 203-212.
- Parche S. 2000. "A fiber model to simulate the cross-sectional behavior of reinforced concrete columns under multi-directional earthquake loading", *Computers and Structures*, 77.
- Priestley, M. J. N. and Park. R. 1987. "Strength and ductility of bridge columns under seismic loading, *ACI Structural Journal*, January-February, pp. 61-76.
- Wang, P. T., Shah, S. P. and Naaman, A. E. 1987. "Stress-strain curves of normal and light weight concrete in compression." *ACI Structural Journal*, 75(62), pp. 603-611.